Published in final edited form as:
Microvasc Res. 2008 April ; 75(3): 403–410. doi:10.1016/j.mvr.2007.12.002.

Endoneurial Microvascular Pathology in Feline Diabetic Neuropathy

Jeannelyn S. Estrella, MD, **Richard N. Nelson, DVM**, **B.K. Sturges, DVM**, **Karen M. Vernau, DVM, MAS**, **D. Collette Williams, BS**, **Richard A. LeCouteur, DVM**, **G. Diane Shelton, DVM, PhD**, and **Andrew P. Mizisin, PhD**
School of Medicine, University of California, San Diego (JSE, GDS, APM) and School of Veterinary Medicine, University of California, Davis (RNN, BKS, KMV, DCW, RAL)

Abstract

Endoneurial capillaries in nerve biopsies from 12 adult diabetic cats with varying degrees of neurological dysfunction were examined for evidence of microvascular pathology and compared to nerves obtained at autopsy from 7 adult non-diabetic cats without clinical evidence of neurological dysfunction. As reported previously (Mizisin et al., 2007), the diabetic cats had elevated glycosylated hemoglobin and serum fructosamine levels, decreased motor nerve conduction velocity and compound muscle action potentials (CMAP), and markedly decreased myelinated nerve fiber densities. Compared to non-diabetic cats, there was a non-significant 26% increase in capillary density and a significant ($P<0.009$) 45% increase in capillary size in diabetic cats. Capillary luminal size was also significantly ($P<0.001$) increased, while an index of vasoconstriction was significantly decreased ($P<0.001$) in diabetic cats compared to non-diabetic controls. No differences in endothelial cell size, endothelial cell number or pericyte size were detected between non-diabetic and diabetic cats. In diabetic cats, basement membrane thickening, seen as a reduplication of the basal lamina, was significantly ($P<0.0002$) increased by 73% compared to non-diabetic controls. Regression analysis of either myelinated nerve fiber density or CMAP amplitude against basement membrane size demonstrated a negative correlation with significant slopes ($P<0.03$ and $P<0.04$, respectively). These data demonstrate that myelinated nerve fiber injury in feline diabetic neuropathy is associated with microvascular pathology and that some of these changes parallel those documented in experimental rodent and human diabetic neuropathy.

Keywords

Basement membrane; Endoneurial capillaries; Endothelial cells; Feline diabetes mellitus; Microangiopathy; Pericytes

INTRODUCTION

As a debilitating complication of diabetes, peripheral neuropathy is a cause of significant morbidity that has no effective therapy and affects up to 50% of diabetic patients (Sima, 2006). The pathogenesis of diabetic peripheral neuropathy is considered to be multifactorial,

Correspondence to: Andrew P. Mizisin, Ph.D., Department of Pathology 0612, School of Medicine, University of California, San Diego, 9500 Gilman Dr., La Jolla CA 92093-0612, Tel: (858) 822-3894, FAX: (858) 534-1886, email: amizisin@ucsd.edu.

with contributions from both metabolic and vascular factors. The importance of microvascular disease has been highlighted by studies in diabetic patients with no (Giannini and Dyck, 1995) or minimal neuropathy (Malik et al., 1992, 2005), where significant endoneurial microangiopathy is present early in the course of the disease. However, the role of microangiopathy in the development of diabetic peripheral neuropathy remains to be elucidated.

One of the major obstacles to research in diabetic neuropathy is the lack of experimental animal models that mimic the pathology apparent in diabetic patients. Capillary basement membrane thickening, the classical pathological feature of diabetic microangiopathy, has only been observed in long-term alloxan-diabetic rats (Powell and Myers, 1984) and recently in acute vacor-induced diabetes, although this change was absent in rats with chronic vacor-induced diabetes (Kim et al., 2002). Further, studies assessing microangiopathy in streptozotocin-diabetic rats (Sugimoto and Yagihashi, 1997; Uehara et al., 1997; Walker et al., 1999; Yasuda et al., 1989), OVE26 transgenic mice (Carlson et al., 2003), and monkeys with long-term streptozotocin diabetes (Sugimoto and Yagihashi, 1997) have failed to demonstrate the range of structural changes in the endoneurial vasculature characteristic of human diabetic neuropathy, including capillary basement membrane thickening with endothelial cell hyperplasia (Giannini and Dyck, 1995; Malik et al., 1989, 1992, 1997, 2005), endothelial cell hypertrophy (Malik et al., 1989, 1993) and pericyte degeneration (Giannini and Dyck, 1994, 1995; Yasuda et al., 1989).

The potential of spontaneously occurring feline diabetes as a suitable animal model has been highlighted by recent studies in our laboratory demonstrating fundamental and remarkable myelinated nerve pathology similar to that in human diabetic neuropathy (Mizisin et al., 2002, 2007). In nerve biopsies from diabetic cats, there is evidence of active and ongoing demyelination and remyelination, as well as axonal degeneration and regeneration, that culminates in myelinated fiber loss in animals with peripheral neuropathy. We now report structural evidence of microangiopathy in these same cat nerves that replicates some of the changes seen in humans, further supporting the potential utility of feline diabetes for studying the pathogenesis of diabetic peripheral neuropathy.

MATERIALS AND METHODS

Adult domestic cats of mixed breeding (9 castrated males and 3 spayed females) with spontaneously occurring, severe insulin-dependent type 2 diabetes mellitus (N = 12) ranging in age from 7 to 15 years were admitted to the Veterinary Medical Teaching Hospital at the University of California, Davis with varying neurological dysfunction. For morphological comparison, common peroneal nerves obtained at autopsy from 7 adult non-diabetic cats without clinical evidence of neurological dysfunction were studied. All studies were performed under an approved protocol of the Institutional Animal Care and Use Committee.

Clinical and Neurophysiologic Data

Complete physical and neurological examinations were performed as described earlier (Mizisin et al., 2007). The neurological examination included observations of mentation, posture and gait, evaluation of segmental spinal reflexes, cranial nerve evaluation and postural reactions. Using previously established criteria for diabetic cats (Mizisin et al. 2002), neurological signs were assigned a numerical severity rank: normal or no deficits (0); very mild (1); mild (2); mild/moderate (3); moderate (4); moderate/severe (5); and severe (6). Criteria associated with the median severity rank of 4 include: irritability when touching and manipulating the feet; a plantigrade posture when standing and walking; mild generalized muscle atrophy; decreased postural reactions; and mildly to moderately decreased tendon reflexes.

Under general inhalation anesthesia, peroneal nerve conduction velocity and compound muscle action potential (CMAP) amplitude were measured in each diabetic cat using a Nicolet Viking IV EMG/evoked potential system (Nicolet, Biomedical Inc, Madison, WI), while maintaining limb and body core temperature above 36°C (Mizisin et al., 2007). For both nerve stimulation and recording from muscle, insulated stainless steel needle electrodes (Nicolet) were used, while a platinum subdermal electrode (Grass-Telefactor, West Warwick, RI) was employed as a ground. After supramaximal stimulation (2 Hz, 0.2 ms), motor nerve conduction velocity (MNCV) was calculated by dividing the distance between proximal and distal stimulation sites by the difference in latency of the corresponding CMAP recorded from plantar interosseous muscles. Amplitude was measured for CMAPs derived from stimulation at the proximal and distal stimulation sites.

For comparison, normal values for non-diabetic cats were derived from normative clinical values or previously published data (body weight from Mizisin et al., 2002; MNCV from Tuler and Bowen 1990; CMAP amplitude from Picavet and Lambillon 1993; and myelinated nerve fiber density from Mizisin et al. 2007).

Histology

Common peroneal nerve specimens, pinned on cork discs to maintain length and orientation, were immersion-fixed in 2.5% glutaraldehyde in 0.1M phosphate buffer before shipment. Upon receipt, the nerves were post-fixed in 1% aqueous osmium tetroxide for 3 to 4 hours (h) before dehydration in a graded alcohol series and propylene oxide. After infiltration with a 1:1 mixture of propylene oxide and araldite resin for 4 h, nerves were placed in 100% araldite resin overnight before embedding in fresh araldite resin. Thick sections (1 μm) were cut with glass knives and stained with toluidine blue prior to light microscopic examination. Thin sections (60–90 nm) were cut with a diamond knife and stained with uranyl acetate and lead citrate before electron microscopic examination.

Endoneurial Vessel Morphometry

Determination of endoneurial capillary density was done using a Jeneval 250-CF light microscope with a camera lucida attachment. The total number of blood vessels from all fascicles were counted and normalized to fascicular area. Only those blood vessels with a clearly defined lumen containing red blood cells and/or associated pericyte profiles were counted. Using point-counting techniques (Weibel, 1979) and a grid with a magnified distance of 0.08 mm between intersection points, fascicular area was estimated by multiplying the area of each grid square by the number of grid intersection points falling within the endoneurium of each fascicle.

Ultrastructural analysis of endoneurial microvasculature was performed using a Zeiss 10 electron microscope operating at 60 keV. Capillaries were defined as blood vessels whose endothelial cells were surrounded by a discontinuous layer of pericyte or smooth muscle cells. All capillaries (range 5–19 per animal) that were unobstructed by grid lines or other artifacts, such as tears, holes and folds, were photographed at a final magnification of X10,000. Composites of multiple negatives were shot for larger vessels that did not fit entirely within a single negative. All measurements were made using point-counting techniques (Weibel, 1979) and a 0.5 cm grid that was superimposed over each negative as it was viewed on a light box. Luminal, endothelial cell, basement membrane and pericyte areas, as shown in Fig. 1a and color-coded in Fig. 1b, were estimated by multiplying the area of each grid square by the number of grid intersection points falling within each corresponding area. Luminal, endothelial cell outer perimeters and pericyte inner perimeters were estimated by counting the number of horizontal and vertical intersections between grid lines and each corresponding perimeter. As illustrated in Fig. 1b, each perimeter = # of intersections × ½ × (π/2 × 0.5 cm).

With area and perimeter measurements, the following variables were determined. Note that endothelial cell outer perimeter was used to normalize measures of basement membrane, endothelial and pericyte areas to capillary size, while luminal perimeter was similarly used to normalize luminal area.

1. Capillary size (μm) = endothelial cell outer perimeter.
2. Basement membrane thickening ($\mu m^2/\mu m$) = basement membrane area divided by capillary size.
3. Endothelial cell hypertrophy ($\mu m^2/\mu m$) = endothelial cell area divided by capillary size.
4. Endothelial cell hyperplasia (# of nuclear profiles) = the number of nuclear profiles.
5. Pericyte cell hypertrophy ($\mu m^2/\mu m$) = pericyte area divided by capillary size.
6. Luminal area ($\mu m^2/\mu m$) = luminal area divided by luminal perimeter.
7. Index of vasoconstriction (VCI) = vessel wall thickness (T) divided by luminal perimeter, with T = (endothelial cell area − luminal area)/(½ × (endothelial cell perimeter + luminal perimeter).

For technical reasons, capillary density was not assessed in 2 diabetic cats and ultrastructural analysis was not performed in 1 non-diabetic cat.

Statistical Analysis

Unless otherwise noted, data are presented as mean ± SD. Differences between morphometric parameters of non-diabetic and diabetic cats were tested using two-tailed, unpaired t-tests. Correlations were analyzed with the Pearson rank-correlation test.

RESULTS

We reported detailed clinical and neurophysiological data, as well as myelinated fiber density, from these diabetic cats in an earlier paper (Mizisin et al., 2007) and summarize them here in Table 1. Briefly, serum glucose was markedly elevated in diabetic cats, with evidence of long-term exposure to hyperglycemia suggested by increased glycosylated hemoglobin and serum fructosamine levels. At the time of biopsy, all cats were receiving insulin to control the diabetic state. Moreover, diabetic cats exhibited some clinical signs of neurological dysfunction (median assessment score of 4, range 2–6 with 0 normal) and weakness, including a plantigrade posture when standing and walking, reluctance to jump and decreased tendon reflexes consistent with lower motor neuron disease. Cats were also irritable when the feet were touched and manipulated. Further, motor neurophysiological function of the common peroneal nerve was markedly impaired, with average MNCV and CMAP amplitude of the diabetic cats less than 50% and 35% of normal values, respectively. There was an obvious loss of myelinated fibers in peroneal nerve biopsies from diabetic cats (Fig. 2), such that average myelinated nerve fiber density in diabetic cats was decreased to 50% of the value in non-diabetic cats.

Qualitatively, the most striking abnormality of endoneurial microvessels was the reduplicated basal lamina present between endothelial cells and pericytes that was consistently present in diabetic (Figs. 1, 3b, 4) but not non-diabetic (Fig. 3a) cats. In some vessels (Fig. 4b), the basal lamina appeared as multiple interconnected segments that had lost a close association with the endothelial cells and pericytes responsible for its production. Conspicuous accumulations of glycogen granules were also noted in the endoneurial blood vessels of diabetic, but not non-diabetic, cats (Figs 1a, 3b, 4a, 4b). These glycogen deposits were present in both endothelial cells (10/12 diabetic cats) and pericytes (12/12 diabetic cats) of nearly all vessels examined.

Lipid droplets were also occasionally observed (Fig. 4a, b) in endothelial cells and pericytes of vessels from diabetic cats, as were electron-dense inclusions in membrane-bound organelles reminiscent of secondary lysosomes (Fig. 4c).

The ultrastructural morphometric analysis of endoneurial microvessels is summarized in Table 2. In diabetic cats, capillary density showed a 26% non-significant increase ($p < 0.06$) over that in non-diabetic animals. Compared to non-diabetic cats, capillary size was increased by 45% ($p < 0.009$) and luminal area by more than 200% ($p < 0.001$) in diabetic cats. The VCI was significantly decreased ($p < 0.001$) by more than 85% in diabetic cats compared to non-diabetic control animals. In diabetic cats, basement membrane thickening, represented by reduplication of the basal lamina (Figs. 1, 3, 4), was significantly increased ($p < 0.0002$) by 73% compared to control animals. There were no differences in endothelial cell hypertrophy, endothelial cell number and pericyte hypertrophy in diabetic and non-diabetic cats. Also, the ratio of inner pericyte perimeter to outer endothelial cell perimeter, an estimate of the amount of endothelial cell surface covered by pericytes, was not different (non-diabetic - 0.27 ± 0.09 and diabetic - 0.26 ± 0.08; mean ± SD, N = 6 and 11, respectively).

DISCUSSION

With respect to deficient insulin secretion, insulin resistance, and pancreatic amyloid deposition (Lutz and Rand, 1995), feline diabetes is similar to type 2 diabetes mellitus in humans and is estimated to be present in up to 2% of the domestic cat population of the United States (Rand et al., 2004). Diabetic cats tend to be overweight and often require insulin for glycemic control (Mizisin et al., 2002), which was the case for the cohort of insulin-dependent diabetic cats studied here (Table 1; Mizisin et al. 2007). Neuropathy in diabetic cats can manifest as a remarkable gait abnormality, characterized by a plantigrade and sometimes palmigrade stance of the limbs that dramatically affects the ability to walk and jump, as well as conduction deficits of motor, sensory and mixed nerves (Mizisin et al., 2002). In addition to decreased peroneal MNCV and CMAP amplitude, similar neurological abnormalities were noted in this study, as diabetic cats were irritable when touching and manipulating feet, often adopted a plantigrade posture when standing and walking, had decreased postural reactions and mildly to moderately decreased tendon reflexes (Table 1; Mizisin et al. 2007). Structural nerve injury in feline diabetic neuropathy ranges from myelin splitting and ballooning, which appears to precede demyelination, to axonal degeneration that, in spite of evidence of remyelination and axonal regeneration, ultimately culminates in myelinated fiber loss, as seen earlier (Mizisin et al., 1998, 2002) and in these diabetic cats (Mizisin et al., 2007). Here, we establish that neuropathy in diabetic cats is also associated with endoneurial microvascular abnormalities, including basement membrane thickening and increased luminal area.

In the peroneal biopsies from the spontaneously diabetic cats examined in this study, the most striking vascular abnormality was the marked basement membrane thickening that manifested as the reduplication of the basal lamina associated with endoneurial vessels (Table 2; Figs. 1, 3, 4). Microvascular pathology has been investigated in experimental diabetes induced by streptozotocin (Kennedy and Zochodne, 2002;Sugimoto and Yagihashi, 1997;Uehara et al., 1997,Walker et al., 1999; Yasuda et al., 1998; Zochodne and Nguyen, 1999), alloxan (Artico et al., 2002;Powell and Myers, 1984) and vacor (Kim et al., 2002), most commonly in the rat but also in the monkey (Yasuda et al., 1989). In these studies, basement membrane thickening has only been observed in long-term (16–18 months) alloxan-induced diabetes (Powell and Myers, 1984) and acute (2 week) vacor-induced diabetes (Kim et al., 2002). Although microangiopathy involves all cellular and noncellular components of the endoneurial microvasculature in human diabetic neuropathy, the most common abnormality is capillary basement membrane thickening (Britland et al., 1990;Giannini and Dyck, 1994,1995;Malik et al., 1989,1992,1993,2005;Sima et al., 1991; Yasida and Dyck, 1987). Similar to feline diabetic

neuropathy, basement membrane thickening in biopsies from human diabetic patients is reflected as reduplication of the basal lamina and thought to be primarily responsible for vessel wall thickening (Britland et al., 1990).

In feline diabetes, two interdependent measures of luminal patency, increased luminal area and a decreased vasoconstriction index, are consistent with the absence of endothelial cell hypertrophy and hyperplasia (Table 2) and may reflect dilation of these capacitance vessels. Because nerve blood flow has not been measured in diabetic cats, it is not clear whether increased luminal area reflects a compensatory response to diabetes-induced ischemia, although it is worth noting that no significant negative correlations between luminal size and indices of nerve function and structure were evident (Table 3). Increased luminal area is also observed in streptozotocin-diabetic rats with duration of diabetes ranging from 3–4 months (Sugimoto and Yagihashi, 1997;Uehara et al., 1997;Yasuda et al., 1989). Whether luminal area of endoneurial vessels is decreased, unchanged or increased at shorter durations of streptozotocin-induced diabetes when nerve blood flow deficits are first apparent (for review see Cameron and Cotter, 1994) is not known, but would be important for establishing whether vessel dilation after 3–4 months of diabetes is a compensatory response to ischemia. In contrast to animal studies, vessel patency appears to be more variable in human diabetic neuropathy, with reports of decreased (Bradley et al., 1990;Dyck et al., 1985;Malik et al., 1993,1994, 2005), unchanged (Giannini and Dyck, 1994;Malik et al., 1992;Sima et al., 1991;Thrainsdottir et al., 2003) or increased (Britland et al., 1990;Malik et al., 1989;Yasuda and Dyck, 1987) luminal area. Capillary closure has been suggested to play a role in the development of diabetic neuropathy (Dyck et al., 1985) and reports of decreased luminal area (Bradley et al., 1990;Malik et al., 1993,1994,2005) may be the morphological basis of reductions in nerve blood flow and consequent hypoxia (Newrick et al., 1986). Because capillary closure has been observed in both non-diabetic and diabetic patients, others suggest that it may be a normal physiological response of capacitance vessels without any pathogenic significance (Sima et al., 1991).

Aside from epineurial arterio-venous shunting (Tesfaye et al., 1996) and the patency of endoneurial vessels, capillary density is a key determinant of nerve perfusion, with a reduction in vascular density and consequent increase in intercapillary distance considered important factors underlying hypoperfusion and hypoxia in diabetic and ischemic neuropathies (Low et al., 1985). The lack of a significant increase in endoneurial capillary density would argue that, in this series of cats, there was no angiogenic response to the consequences of diabetes, which is supported by the positive, not negative, correlation between capillary density and CMAP, a measure of neurophysiological function (Table 3). In experimental diabetes, increases in endoneurial capillary density have been reported (Artico et al., 2002; Uehara et al., 1997), but more commonly angiogenesis is absent (Sugimoto and Yagihashi, 1997; Zochodne and Nguygen, 1989), especially in diabetes of longer duration (Kennedy and Zochodne, 2002), or present only when whole (epineurium plus endoneurium) nerve is considered (Zochodne and Nguyen, 1999). In human diabetic neuropathy, changes in capillary density have not been reported in patients with established neuropathy (Britland et al., 1990; Giannini and Dyck, 1994; Malik et al., 2005; Thrainsdottir et al., 2003), whereas a reduction in endoneurial capillary density was observed in patients with clinically mild neuropathy (Malik et al., 1992), and increased capillary density was shown to precede the development of diabetes in those with impaired glucose tolerance (Thrainsdottir et al., 2003).

The absence of endothelial cell or pericyte degeneration in feline diabetic neuropathy suggests that basal lamina reduplication results from functional, not structural, disorders of these cells, as has been suggested for human diabetic neuropathy based on the observation that reduplication is present before degenerative cellular changes (Giannin and Dyck, 1995). Given that basement membrane thickening is infrequent in experimental diabetes, it is perhaps not

surprising that hypertrophy and/or hyperplasia of endothelial cells and/or pericytes is not common, with just a single report of endothelial proliferation in long-term alloxan-diabetic rats (Powell and Myers, 1984). In sural nerve biopsies from diabetic patients, endothelial hypertrophy and hyperplasia are commonly reported (Malik et al., 1989, 1992, 1993, 1994, 2005; Yasuda and Dyck, 1987), with pericyte degeneration noted occasionally (Giannin and Dyck, 1994, 1995; Yasuda and Dyck, 1987), which is likely a reflection of the duration and severity of diabetes.

Evidence indicating a role for microvascular alterations in the pathogenesis of human diabetic neuropathy derive from correlations of endoneurial capillary pathology with neurophysiological and morphological assessments of the severity of neuropathy (Britland et al., 1990; Malik et al., 1989, 1993). Further, microvascular pathology has been observed in diabetic patients with no (Giannini and Dyck, 1995) or minimal (Malik et al., 1992, 2005) neuropathy, suggesting that injury to vessels precedes nerve fiber loss and supporting an ischemic mechanism for human diabetic neuropathy. In the diabetic cats studied here, regression analysis indicated that CMAP and myelinated nerve fiber density were indirectly related to basement membrane thickening and directly related to capillary density (Table 3). Thus, both morphological and neurophysiological indices of neuropathy are correlated with basement membrane thickening, one of the hallmarks of diabetic microangiopathy. However, unlike human diabetic neuropathy, myelinated nerve fiber injury in feline diabetic neuropathy (Mizisin et al., 2007) is coexistent with microvascular pathology that is limited to basement membrane thickening without endothelial cell and pericyte degeneration. Thus, the magnitude and temporal expression of microvascular pathology does not offer strong support for an ischemic mechanism for feline diabetic neuropathy, arguing for the contribution of other mechanisms (for review see Wada and Yagihashi, 2005).

In conclusion, the microvascular pathology observed in common peroneal nerve biopsies from the 12 diabetic cats studied here further augment previously reported neuropathological findings (Mizisin et al., 2007). The key finding, basement membrane thickening, occurs in the context of significant neurological and neurophysiological deficits as well as extensive Schwann cell and axonal injury, and is negatively correlated with CMAP amplitude and myelinated nerve fiber density. Myelinated nerve fiber injury in feline diabetic neuropathy is associated with microvascular pathology that parallels some, but not all, of the changes documented in human diabetic neuropathy. The appearance of myelinated nerve fiber and microvascular pathology suggests that feline diabetes mellitus is a promising animal model, although the following potential limitations may restrict its utility and warrant further consideration. The study of the pre-diabetic and early diabetic state is complicated because the time between onset and diagnosis of feline diabetes mellitus is variable, as many owners do not seek veterinary assistance until after their pet has developed severe insulin-dependent diabetes. As with human diabetic neuropathy, interpretation of neuropathological findings should consider the potential impact of the neurotrophic effects of insulin, as most diabetic cats are treated with insulin due to the severity of diabetes when treatment is initiated. Finally, the influence of neutering on the development of nerve injury in feline diabetes is unknown, although most pet cats are neutered by 12 to 16 weeks in the United States and none develop the clinical manifestations of diabetic neuropathy.

Acknowledgements

This work was conducted with support from Blue Ridge Pharmaceuticals (currently a subsidiary of IDEXX Inc.), Greensboro, NC, USA, the Center for Companion Animal Health, School of Veterinary Medicine, University of California, Davis, CA, USA, the Juvenile Diabetes Research Foundation and NIH grant DK078374.

References

Artico M, Massa R, Cavollotti D, Franchitto S, Cavallotti C. Morphological changes in the sciatic nerve of diabetic rats treated with low molecular weight heparin OP 2123/Parnaparin. Anat Histol Embryol 2002;31:193–197. [PubMed: 12196260]

Bradley J, Thomas PK, King RHM, Llewelyn JG, Muddle JR, Watkins PJ. Morphometry of endoneurial capillaries in diabetic sensory and autonomic neuropathy. Diabetologia 1990;33:611–618. [PubMed: 2257998]

Britland ST, Young RJ, Sharma AK, Clarke BF. Relationship of endoneurial capillary abnormalities to type and severity of diabetic polyneuropathy. Diabetes 1990;39:909–913. [PubMed: 2373263]

Cameron NE, Cotter MA. The relationship of vascular changes to metabolic factors in diabetes mellitus and their role in the development of peripheral nerve complicatiosn. Diabetes Metab Rev 1994;10:189–234. [PubMed: 7835170]

Carlson EC, Audette JL, Veitenheimer NJ, Risan JA, Laturnus DI, Epstein PN. Ultrastructural morphometry of capillary basement membrane thickness in normal and transgenic diabetic mice. Anat Rec A Discov Mol Cell Evol Biol 2003;271:332–341. [PubMed: 12629676]

Dyck PJ, Hansen S, Karnes J, O'Brien P, Yasuda H, Windebank A, Zimmerman B. Capillary number and percentage closed in human diabetic sural nerve. Proc Natl Acad Sci USA 1985;82:2513–2517. [PubMed: 3857597]

Giannini C, Dyck PJ. Ultrastructural morphometric abnormalities of sural nerve endoneurial microvessels in diabetes mellitus. Ann Neurol 1994;36:408–415. [PubMed: 8080248]

Giannini C, Dyck PJ. Basement membrane reduplication and pericyte degeneration precede development of diabetic polyneuropathy and are associated with its severity. Ann Neurol 1995;37:498–504. [PubMed: 7717686]

Kennedy JM, Zochodne DW. Influence of experimental diabetes on the microcirculation of injured peripheral nerve. Functional and morphological aspects. Diabetes 2002;51:2233–2240. [PubMed: 12086955]

Kim J, Lee TH, Lee MC, Moon JD, Lee JS, Kim HS, Suh CH. Endoneurial microangiopathy of sural nerve in experimental vacor-induced diabetes. Ultrastruct Pathol 2002;26:393–401. [PubMed: 12537764]

Low PA, Lagerlund TD, McManis PG. Nerve blood flow and oxygen delivery in normal, diabetic, and ischemic neuropathy. Int Rev Neurobiol 1985;31:355–438. [PubMed: 2557297]

Lutz TA, Rand JS. Pathogenesis of feline diabetes mellitus. Vet Clin North Am Small Anim Pract 1995;25:527–552. [PubMed: 7660530]

Malik RA. The pathology of human diabetic neuropathy. Diabetes 1997;46(Suppl2):S50–S53. [PubMed: 9285499]

Malik RA, Newrick PG, Sharma AK, Jennings A, Ah-See AK, Mayhew TM, Jakubowski J, Boulton AJ, Ward JD. Microangiopathy in human diabetic neuropathy: relationship between capillary abnormalities and the severity of neuropathy. Diabetologia 1989;32:92–102. [PubMed: 2721843]

Malik RA, Tesfaye S, Newrick PG, Walker D, Rajbhandari SM, Siddique I, Sharma AK, Boulton AJM, King RHM, Thomas PK, Ward JD. Sural nerve pathology in diabetic patients with minimal but progressive neuropathy. Diabetologia 2005;48:578–585. [PubMed: 15729579]

Malik RA, Tesfaye S, Thompson SD, Veves A, Hunter A, Sharma AK, Ward JD, Boulton AJ. Transperineurial capillary abnormalities in the sural nerve of patients with diabetic neuropathy. Microvasc Res 1994;48:236–245. [PubMed: 7854207]

Malik RA, Tesfaye S, Thompson SD, Veves A, Sharma AK, Boulton AJ, Ward JD. Endoneurial localization of microvascular damage in human diabetic neuropathy. Diabetologia 1993;36:454–459. [PubMed: 8314451]

Malik RA, Veves A, Masson EA, Sharma AK, Ah-See AK, Schady W, Lye RH, Boulton AJ. Endoneurial capillary abnormalities in mild human diabetic neuropathy. J Neurol Neurosurg Psychiat 1992;55:557–561. [PubMed: 1640230]

Mizisin AP, Nelson RW, Sturges BK, Vernau KM, LeCouteur RA, Williams DC, Burgers ML, Shelton GD. Comparable myelinated nerve pathology in feline and human diabetes mellitus. Acta Neuropathol 2007;113:431–442. [PubMed: 17237938]

Mizisin AP, Shelton GD, Burgers ML, Powell HC, Cuddon PA. Neurological complications associated with spontaneously occurring feline diabetes mellitus. J Neuropathol Exp Neurol 2002;61:872–884. [PubMed: 12387453]

Mizisin AP, Shelton GD, Wagner S, Rushbridge C, Powell HC. Myelin splitting, Schwann cell injury and demyelination in feline diabetic neuropathy. Acta Neuropathol 1998;95:171–174. [PubMed: 9498053]

Newrick PG, Wilson AJ, Jakubowski J, Boulton AJ, Ward JD. Sural nerve oxygen tension in diabetes. Br Med J 1986;293:1053–1054. [PubMed: 3094772]

Picavet PM, Lambillon DE. Motor nerve conduction in the cat's hind limb. Prog Vet Neurol 1993;4:121–125.

Powell HC, Myers RR. Axonapathy and microangiopathy in chronic alloxan diabetes. Acta Neuropathol 1984;65:128–137. [PubMed: 6098120]

Rand JS, Fleeman LM, Farrow HA, Appleton DJ, Lederer R. Canine and feline diabetes mellitus: nature or nuture? J Nutr 2004;134:2072S–2080S. [PubMed: 15284406]

Sima AA. Pathological mechanisms involved in diabetic neuropathy: can we slow the process. Curr Opin Invest Drugs 2006;7:324–337.

Sima AA, Nathaniel V, Prashar A, Bril V, Greene DA. Endoneurial microvessels in human diabetic neuropathy. Endothelial cell dysjunction and lack of treatment effect by aldose reductase inhibitor. Diabetes 1991;40:1090–1099. [PubMed: 1936616]

Sugimoto K, Yagihashi S. Effects of aminoguanidine on structural alterations of microvessels in peripheral nerve of streptozotocin diabetic rats. Microvasc Res 1997;53:105–112. [PubMed: 9143541]

Tesfaye S, Malik R, Harris N, Jakubowski JJ, Mody C, Rennie IG, Ward JD. Arterio-venous shunting and proliferating new vessels in acute painful neuropathy of rapid glycaemic control (insulin neuritis). Diabetologia 1996;39:329–335. [PubMed: 8721779]

Thrainsdottir S, Malik RA, Dahlin LB, Wiksell P, Eriksson KF, Rosen I, Petersson J, Greene DA, Sundkvist G. Endoneurial capillary abnormalities presage deterioration of glucose tolerance and accompany peripheral neuropathy in man. Diabetes 2003;52:2615–2622. [PubMed: 14514647]

Tuler SM, Bowen JM. Measurement of conduction velocity of the peroneal nerve based on recordings from extensor digitorum brevis muscle. J Am Anim Hosp Assoc 1990;26:164–168.

Uehara K, Sugimoto K, Wada R, Yoshikawa T, Marukawa K, Yasuda Y, Kimura Y, Yagihashi S. Effects of cilostazol on the peripheral nerve function and structure in STZ-induced diabetic rats. J Diabetes Complications 1997;11:194–202. [PubMed: 9174902]

Wada R, Yagahashi S. Role of advanced glycation end products and their receptors in development of diabetic neuropathy. Ann NY Acad Sci 2005;1043:598–604. [PubMed: 16037282]

Walker D, Carrington A, Cannan SA, Sawicki D, Sredy J, Boulton AJ, Malik RA. Structural abnormalities do not explain the early functional abnormalities in the peripheral nerves of the streptozotocin diabetic rat. J Anat 1999;195:419–427. [PubMed: 10580857]

Weibel, ER. Stereological Methods. Academic Press; New York: 1979.

Yasuda H, Dyck PJ. Abnormalities of endoneurial microvessels and sural nerve pathology in diabetic neuropathy. Neurology 1987;37:20–28. [PubMed: 3796834]

Yasuda H, Sonobe M, Yamashita M, Terada M, Hatanaka I, Huitan Z, Shigeta Y. Effect of prostaglandin E1 analogue TFC 612 on diabetic neuropathy in streptozotocin-induced diabetic rats. Comparison with aldose reductase inhibitor ONO 2235. Diabetes 1989;38:832–838. [PubMed: 2525492]

Yasuda H, Taniguichi Y, Huitan Z, Kosugi K, Hidaka H, Hatanaka I, Kashiwagi A, Kikkawa R, Harano Y, Shigeta Y. Chronically streptozotocin-diabetic monkey does not closely mimic human diabetic neuropathy. Exp Neurol 1989;104:133–137. [PubMed: 2523314]

Zochodne DW, Nguyen C. Increased peripheral nerve microvessels in early experimental diabetic neuropathy: quantitative studies of nerve and dorsal root ganglia. J Neurol Sci 1999;166:40–46. [PubMed: 10465498]

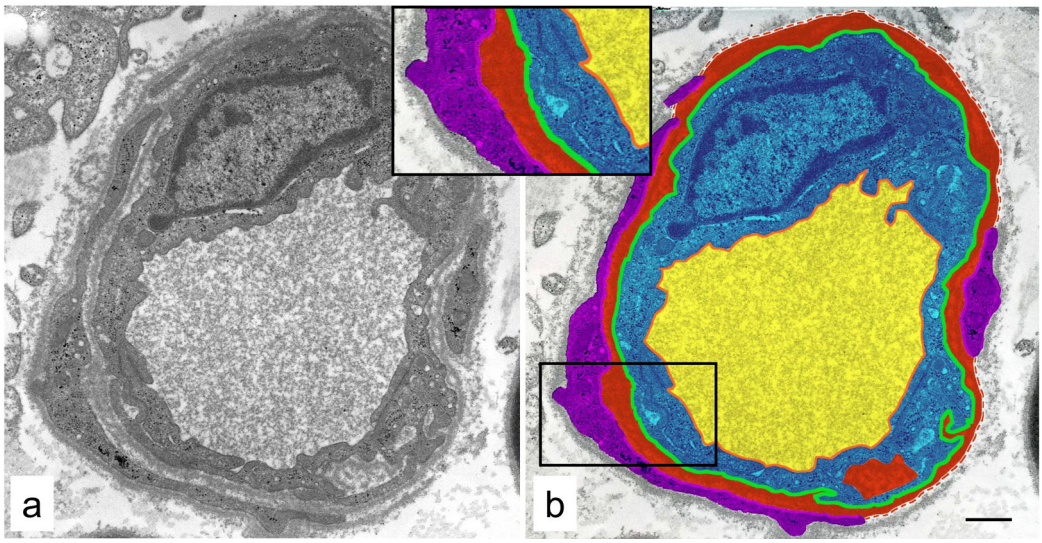

Fig. 1.

Endoneurial blood vessel from a diabetic cat (**a**) with areas and perimeters used for morphometric measurements designated on this vessel by color code (**b**) as follows: luminal area - *yellow*; endothelial cell area - *blue*; basement membrane area - *red*; pericyte area - *purple*; luminal perimeter -*orange*; outer endothelial cell perimeter - *green*; and inner pericyte perimeter -*pink*. Dashed red line denotes outer extent of basement membrane not enclosed by pericyte processes. Inset shows region outlined in (**b**). *Bar* 1.5 μm.

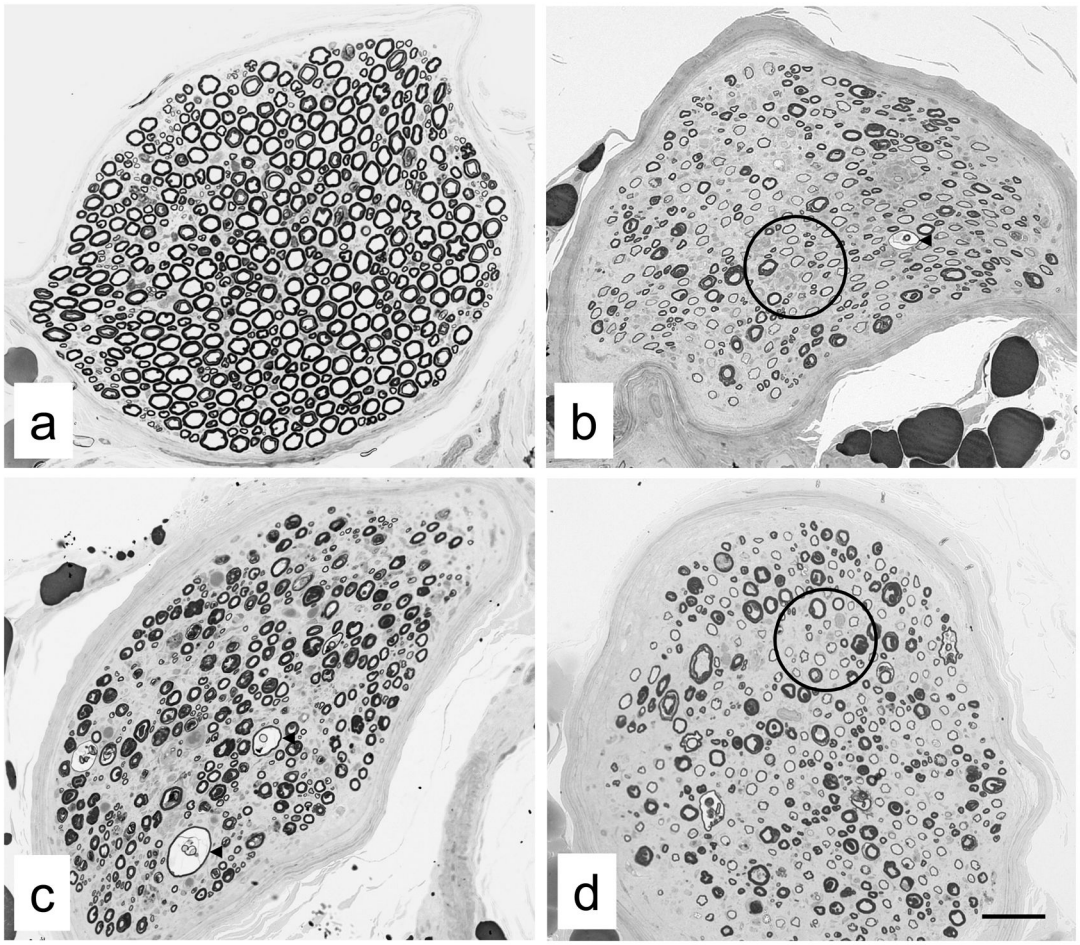

Fig. 2.

Examples of peroneal nerve biopsies from non-diabetic (**a**) and diabetic (**b**-**d**) cats from which endoneurial blood vessels were sampled. Note myelinated fiber density of peroneal nerve fascicles in non-diabetic cat (**a**) and the obvious myelinated fiber loss evident in diabetic cats (**b**-**d**). In diabetic cats, evidence of active demyelination was indicated by fibers with split and ballooned myelin sheaths (*arrowheads* in **b** and **c**), while remyelination was suggested by fibers with disproportionately thin myelin sheaths (*circles* in **b** and **d**) relative to those of fibers with comparable axonal diameters. *Bar* 73 μm (**a**), 46 μm (**b**), 55 μm (**c**) and 58 μm (**d**).

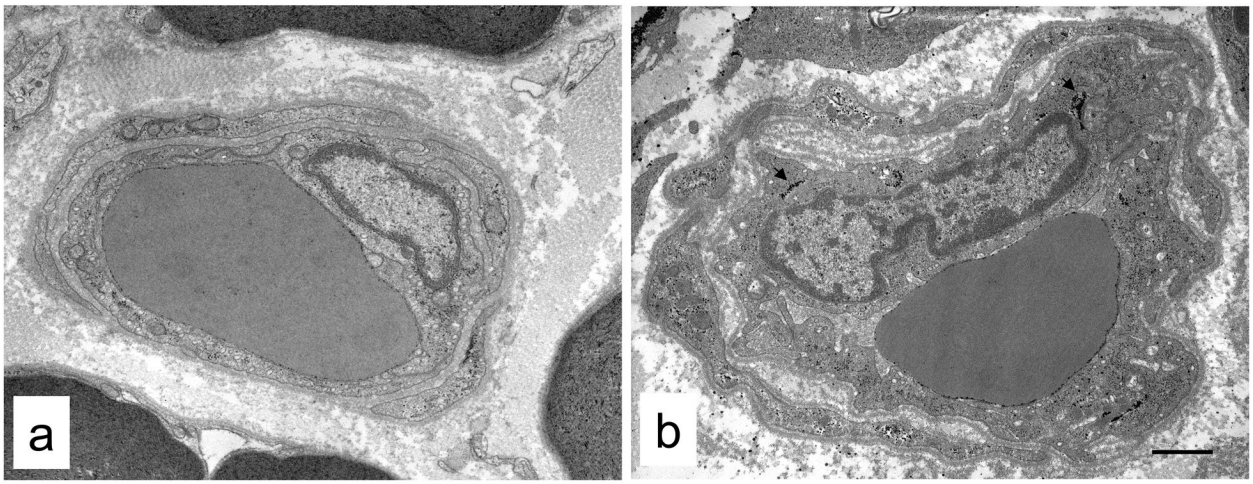

Fig. 3.

Representative endoneurial blood vessels from non-diabetic (**a**) and diabetic (**b**) cats. The most obvious difference was the presence of reduplicated basement membrane between the endothelium and pericytes in the vessel from the diabetic cat. Note also increased glycogen deposition in the endothelium (*arrowheads*). *Bar* 1.3 μm (**a**) and 1.2 μm (**b**).

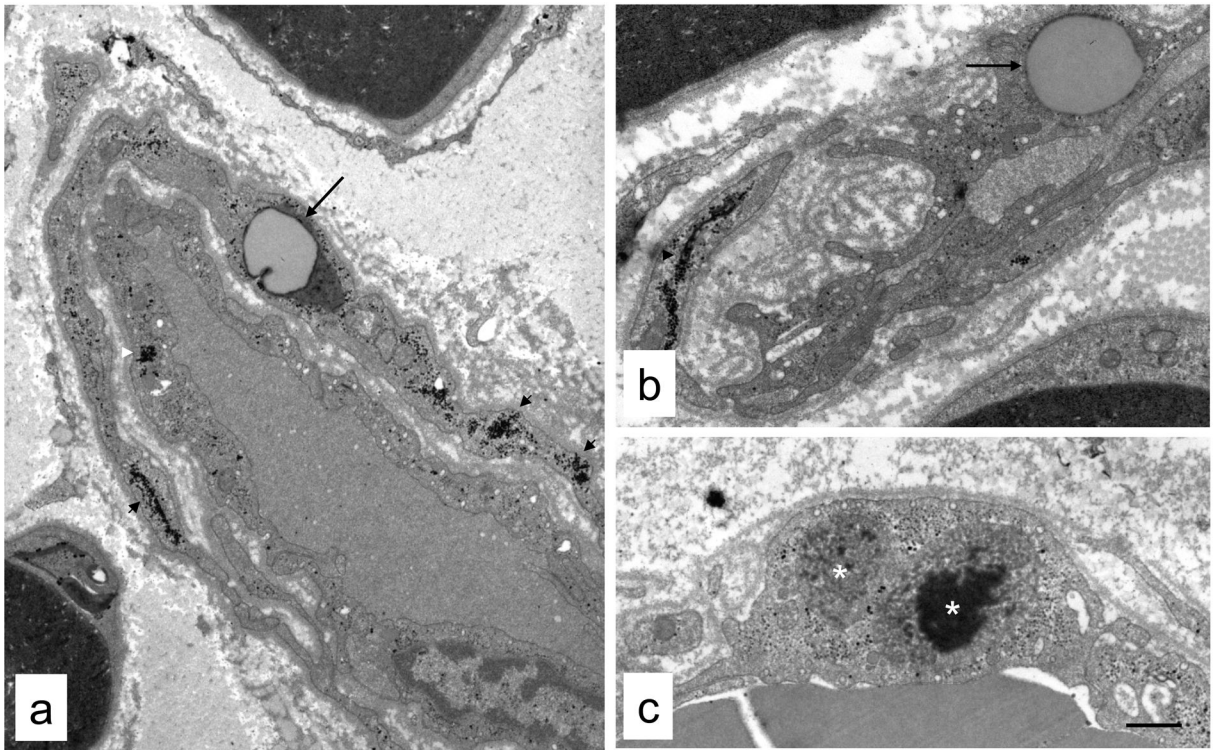

Fig. 4.

Ultrastructural pathology in endoneurial vessels from diabetic cats. Reduplicated basement membrane was evident between endothelial cells and surrounding pericytes (**a**, **b**). Large numbers of glycogen granules (*arrowheads*) were also apparent in endothelial cells and pericytes, as well as lipid accumulation in these cells (*arrows*). Electron-dense inclusions within membrane-bound organelles (*white asterisks*), possibly secondary lysosomes, were also visible in some endothelial cells (**c**) and pericytes. *Bar* 1.5 μm (**a**), 1.3 μm (**b** and **c**).

Table 1

Clinical data, neurological assessment, common peroneal nerve motor function and myelinated nerve fiber density of diabetic cats

	Diabetic cats	Normal values
Sex (male/female)	9/3	-
Age (years)	11 (7–15)	-
Weight (kg)	5.6 ± 0.3	4.5 ± 0.4[A]
Glycosylated Hb (%)	2.9 ± 0.2	0.9–2.5
Serum glucose (mg/dl)	292 ± 48	70–150
Serum fructosamine (mol/l)	525 ± 29	190–360
Neurological score	4 (2–6)	0
Motor nerve conduction velocity (m/s)	43 ± 4	89 ± 3[B]
Compound muscle action potential (mV)	5.7 ± 1.5	16.4 ± 0.6[C]
Myelinated nerve fiber density (#/mm^2)	5,782 ± 514	11,517 ± 1,150[D*]

Data from diabetic cats are presented as median (range), mean ± SEM or range. With the exception of myelinated nerve fiber density, normal values are derived from previously published data or normative clinical values:

[A](Mizisin et al., 2002),

[B](Tuler and Bowen, 1990),

[C](Picavet and Lambillon, 1993) and

[D](Mizisin et al., 2007). Normal values for myelinated nerve fiber density were derived from common peroneal nerves taken at necropsy from non-diabetic cats without evidence of neurological dysfunction.

[*] $P < 0.0001$ (two-tailed unpaired t-test).

Table 2

Morphometric assessment of endoneurial microvasculature in the common peroneal nerve from non-diabetic and diabetic cats

	Non-diabetic	Diabetic	P Value
Capillary density (#/mm^2)	128 ± 35	162 ± 33	0.06
Capillary size (μm)	24.1 ± 2.7	34.9 ± 8.4	0.009
Endothelial cell hypertrophy (μm^2/μm)*	0.52 ± 0.05	0.51 ± 0.09	0.83
Endothelial cell nuclei (#/vessel)	0.8 ± 0.2	0.9 ± 0.3	0.39
Pericyte hypertrophy (μm^2/μm)*	0.27 ± 0.09	0.26 ± 0.08	0.8
Basement membrane thickening (μm^2/μm)*	0.11 ± 0.03	0.19 ± 0.03	0.0002
Luminal area (μm^2/μm)*	0.28 ± 0.13	0.65 ± 0.20	0.001
Vasoconstriction index	0.051 ± 0.030	0.007 ± 0.015	0.001

Data are presented as mean ± SD (N = 6–7 for non-diabetic and 10–12 for diabetic cats) and were compared using an unpaired, two-tailed t-test.

*Note that encdothelial cell outer perimeter or luminal perimeter were used to normalize endothelial cell, pericyte, basement membrane and luminal areas to capillary size to derive the reported measures of endothelial cell hypertrophy, pericyte hypertrophy, basement membrane thickening and luminal area.

Table 3

Coefficients of determination (R^2) for regressions of MNCV, CMAP and myelinated nerve fiber density (dependent variables) against capillary density, capillary size, basement membrane thickening, luminal size and VCI (independent variables) for diabetic cats*

	MNCV	CMAP	MNFD
Capillary density	0.320	0.454[A]	0.233
Capillary size	0.042	0.012	0.091
Basement membrane thickening	0.160	0.381[B]	0.432[C]
Luminal size	0.222	0.001	0.102
Vasoconstriction index	0.286	0.040	0.032

* Regressions with statistically significant slopes are denoted with superscripts as follows:

[A] $P < 0.05$, positive slope;

[B] $P < 0.04$, negative slope;

[C] $P < 0.03$, negative slope.

Abbreviations: MNCV = motor nerve conduction velocity; CMAP = compound muscle action potential; MNFD = myelinated nerve fiber density.